LOCKHEED MARTIN ENERGY RESEARCH LIBRARIES
3 4456 0515078 8

CENTRAL RESEARCH LIBRARY
DOCUMENT COLLECTION

cy 1

ORNL-4739
UC-25 – Metals, Ceramics, and Materials

THE EFFECT OF OXYGEN IN STATIC SODIUM ON VANADIUM AND VANADIUM ALLOYS

R. L. Klueh
J. H. DeVan

OAK RIDGE NATIONAL LABORATORY
CENTRAL RESEARCH LIBRARY
DOCUMENT COLLECTION
LIBRARY LOAN COPY
DO NOT TRANSFER TO ANOTHER PERSON
If you wish someone else to see this document, send in name with document and the library will arrange a loan.
UCN-7969
(3 3-67)

OAK RIDGE NATIONAL LABORATORY
operated by
UNION CARBIDE CORPORATION
for the
U.S. ATOMIC ENERGY COMMISSION

Printed in the United States of America. Available from
National Technical Information Service
U.S. Department of Commerce
5285 Port Royal Road, Springfield, Virginia 22151
Price: Printed Copy $3.00; Microfiche $0.95

This report was prepared as an account of work sponsored by the United States Government. Neither the United States nor the United States Atomic Energy Commission, nor any of their employees, nor any of their contractors, subcontractors, or their employees, makes any warranty, express or implied, or assumes any legal liability or responsibility for the accuracy, completeness or usefulness of any information, apparatus, product or process disclosed, or represents that its use would not infringe privately owned rights.

ORNL-4739

Contract No. W-7405-eng-26

METALS AND CERAMICS DIVISION

THE EFFECT OF OXYGEN IN STATIC SODIUM ON VANADIUM AND VANADIUM ALLOYS

R. L. Klueh and J. H. DeVan

NOVEMBER 1971

OAK RIDGE NATIONAL LABORATORY
Oak Ridge, Tennessee 37830
operated by
UNION CARBIDE CORPORATION
for the
U.S. ATOMIC ENERGY COMMISSION

LOCKHEED MARTIN ENERGY RESEARCH LIBRARIES

3 4456 0515078 8

CONTENTS

Page

Abstract 1

Introduction 1

Experimental 3

Results 6

Unalloyed Vanadium 6

Vanadium Alloys 10

Discussion 19

Unalloyed Vanadium 19

Vanadium Alloys 21

Summary and Conclusions 33

Acknowledgments 34

References 35

THE EFFECT OF OXYGEN IN STATIC SODIUM ON VANADIUM AND VANADIUM ALLOYS

R. L. Klueh and J. H. DeVan

ABSTRACT

Static capsule tests were used to investigate the effect of oxygen in sodium on vanadium and vanadium alloys. When unalloyed vanadium in a vanadium capsule was exposed at 600 and 800°C to sodium that contained up to 1500 ppm O, the specimen and capsule gettered all the oxygen. Vanadium specimens were also exposed to sodium containing up to 4000 ppm O at 600°C in capsules of type 304L stainless steel and molybdenum. Except when the sodium contained over 2000 ppm O, all oxygen was gettered. We concluded that the oxygen distribution coefficient between vanadium and sodium, that is, the ratio of the oxygen concentration in the vanadium to that in the sodium, at equilibrium, is greater than 10^4.

To compare the effect of oxygen in sodium on various vanadium alloys with that on unalloyed vanadium, specimens of the alloys and unalloyed vanadium were simultaneously exposed to sodium containing 2000 ppm O. Alloys tested were: V–5% Cr, V–10% Cr, V–15% Cr, V–20% Ti, V–15% Cr–5% Ti, V–1.3% Zr, V–5% Zr, V–20% Mo, Vanstar 7, Vanstar 8, and Vanstar 9. The results on the alloys can be divided into two groups: alloys that formed internal oxides and those that did not. Of the alloys tested, only the chromium alloys and the V–20% Mo did not form internal oxides. Both chromium and molybdenum lowered the solubility of oxygen in vanadium, results that were explained in terms of the effect of chromium and molybdenum on the activity coefficient of oxygen in vanadium. The remainder of the alloys contain dissolved titanium or zirconium, which precipitate oxides when oxygen is gettered by these materials. Observations on the internally oxidized alloys are discussed in terms of existing internal oxidation theory.

INTRODUCTION

Because vanadium and several vanadium alloys have favorable nuclear cross sections, good fabricability, excellent high-temperature mechanical properties, resistance to high-temperature radiation damage, and

compatibility with nuclear fuels, they are being considered as possible nuclear fuel cladding materials for a Liquid-Metal Fast Breeder Reactor (LMFBR). Since the cladding will be exposed to a liquid sodium coolant, a major part of the testing of vanadium alloys has concerned their compatibility with sodium at 500 to 800°C. The results from various corrosion studies on vanadium alloys are in qualitative agreement and show that compatibility depends strongly on the oxygen concentration of the sodium.[1–4]

When exposed to hot-trapped sodium (i.e., sodium purified by continuous passage over a heated active metal, e.g., zirconium chips at 600°C), vanadium and vanadium alloys show small weight gains that are attributed to oxygen absorption. In cold-trapped sodium (sodium is cold trapped by passing it through a low-temperature zone to precipitate sodium oxide) vanadium and vanadium alloys usually show heavy weight losses due to the formation and spallation of nonadherent surface scales. In cold-trapped systems, oxygen is also absorbed by the matrix, but the weight thus gained is negligible compared to the weight lost by scale spallation.

The oxygen absorbed by the matrix is in one of two forms, depending on the alloying elements:[5] for unalloyed vanadium and vanadium alloyed with elements that form less stable oxides than vanadium, the oxygen is in solid solution; for alloying elements that form more stable oxides than vanadium, the absorbed oxygen forms an oxide precipitate of the alloying component (i.e., internal oxidation occurs).

Internal oxidation of vanadium-titanium and vanadium-aluminum alloys leads to the formation of a "hardened zone" immediately below the external surface in the absence of an external scale, and immediately below the scale when one is present.[1–4] The depth of the hardened zone, which is the extent of internal oxidation, increases with time.[1–4] We previously showed[5] that internal oxidation of vanadium-titanium alloys in sodium follows the kinetics derived by Wagner[6] when no external scale forms and that by Rapp and Colson[7] when internal oxidation occurs along with external scale formation.

In this report we discuss an investigation of the effect of oxygen in sodium on vanadium and vanadium alloys using a series of static capsule experiments. The object was to determine the effect of oxygen in sodium

on the compatibility of vanadium with sodium and to determine the role of various alloying elements on the compatibility.

EXPERIMENTAL

Two types of static capsule tests were run. In the first experiments, where the object was the determination of the effect of oxygen in sodium on vanadium, commercial vanadium was tested in vanadium capsules of the type shown schematically in Fig. 1; Table 1 lists the starting compositions for the 0.04-in. vanadium sheet used to make the specimens and the vanadium tubing used for capsule material. A vanadium specimen was in contact with the sodium in a vanadium capsule, which, in turn, was encapsulated in a protective stainless steel container (Fig. 1).

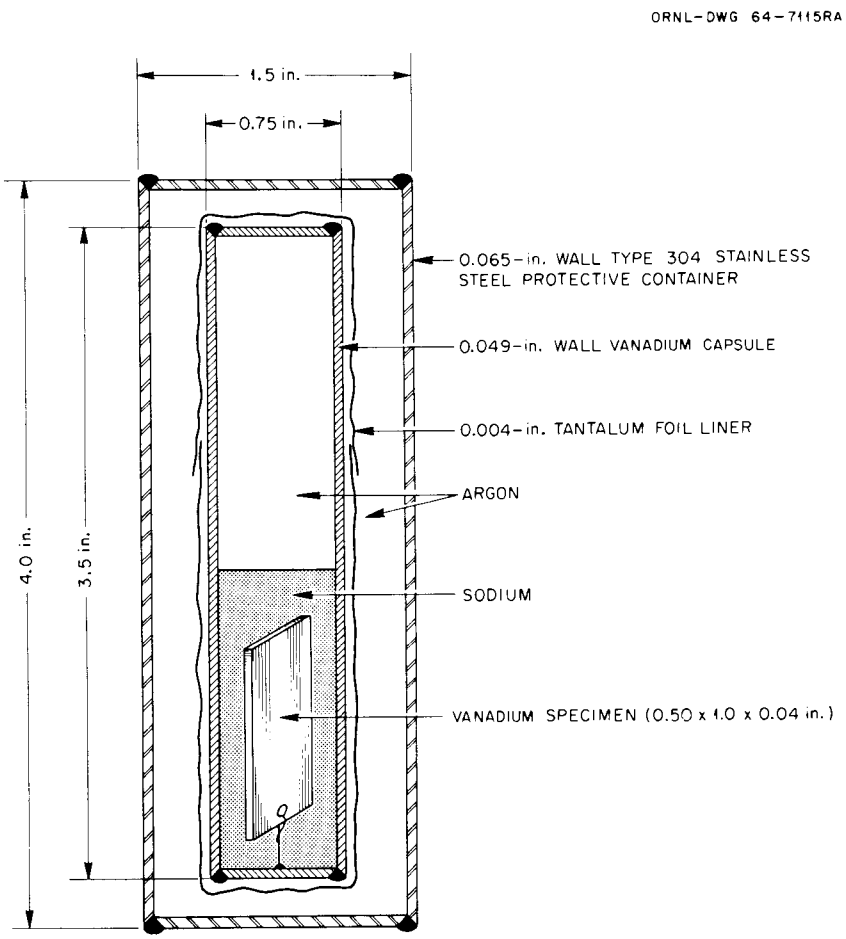

Fig. 1. Schematic Drawing of Corrosion Test Capsule Used to Study Oxygen Effects in Vanadium-Sodium System.

Table 1. Chemical Analysis of Vanadium Used in Vanadium-Sodium Experiments

Impurity Element	Concentration,[a] ppm	
	Tubing	Sheet
O	1300, 1600	1900
H	2, 10	< 1
N	500, 580	570
C	170, 180	470
Ni	< 10	100
Si	80	80
Ti	40	20
Zr	10	20
Cr	< 4	40
Cu	10	20
Fe	200	500
Mg	20	40
Mn	4	80

[a]Two values indicate duplicate determinations.

Tests were conducted at 600 and 800°C for times up to 600 hr. The oxygen concentration of the sodium was varied by weighed additions of Na_2O. In addition, two series of the 600°C tests were conducted with molybdenum and type 304L stainless steel capsules.

In the second type of test, the object was to compare the effect of oxygen in sodium on various alloys with the effect on unalloyed vanadium at 600°C. In these tests a capsule design similar to Fig. 1 was used, but two specimens – the alloy being tested along with a specimen of unalloyed vanadium – were simultaneously exposed to sodium that contained 2000 ppm O in a capsule of type 304L stainless steel. Stainless steel was used because the tests on unalloyed vanadium showed little mass transfer between stainless steel and vanadium at 600°C. The alloys tested were:* V–5% Cr, V–10% Cr, V–15% Cr, V–20% Ti, V–15% Cr–5% Ti, V–1.3% Zr, V–5% Zr, V–20% Mo, Vanstar† 7 (V–9% Cr–3% Fe–1.3% Zr–0.05% C), Vanstar 8 (V–8% Cr–10% Ta–1.3% Zr–0.05% C), and Vanstar 9 (V–6% Fe–5% Nb–1.3% Zr–0.05% C).

*Compositions are in percent by weight.

†Vanstar is a Westinghouse trade designation.

Table 2 lists the actual compositions of the alloys along with the amounts of interstitial impurities present. The vanadium specimens for these tests were made from special high-purity material obtained from the U.S. Bureau of Mines that was melted, cast, and rolled to 0.04-in. sheet (Table 2). This same vanadium was used for making the V-Cr, V-Zr, and V-Mo alloys. The V–20% Ti, V–15% Cr–5% Ti, and the Vanstar alloys were obtained from Westinghouse Astronuclear Laboratory as 0.04-in. sheet.

Table 2. Chemical Analysis of Vanadium and Vanadium Alloys Used in Comparative Tests

	Content, wt %							Content, wt ppm		
	Cr	Ti	Zr	Mo	Fe	Nb	Ta	C	O	N
V								70	80	8
V–5% Cr	5.41							80	120	60
V–10% Cr	9.92							140	90	55
V–15% Cr	14.4							60	150	10
V–15% Cr–5% Ti	14.9	5.0						90	890	90
V–20% Ti		19.7						130	830	80
V–1.3% Zr			1.35					110	130	40
V–5% Zr			4.64					150	210	45
V–20% Mo				20.5				70	150	60
Vanstar 7	9.4		1.2		3.3			640	1000	90
Vanstar 8	8.4		1.1				8.9	570	900	90
Vanstar 9			1.2		6.2	5.2		600	1000	95

Specimens 1 × 3/8 × 0.04 in. were used for all tests and were vacuum annealed for 1 hr at 900°C. Since vanadium and sodium react with air, all loading and welding operations were carried out in an argon atmosphere chamber. The capsules were heated to the test temperature in the inverted position, then rotated at temperature to expose the specimen to the sodium. After test the capsules were inverted and quenched into liquid nitrogen. The oxygen concentration of the specimens and capsules (both before and after test) was determined by either vacuum fusion or

fast-neutron activation analysis. For those tests where the after-test vanadium concentration of the sodium was determined, the sodium was dissolved in isopropyl alcohol and recovered from it as sodium fluoride; then the amount of vanadium in the sodium fluoride was determined by spectrographic analysis.

RESULTS

Unalloyed Vanadium

The first tests consisted of a series of static capsule tests designed to measure the oxygen partitioning between unalloyed vanadium and sodium and compare the effect of oxygen in sodium on vanadium with our previously reported[8] findings on the effect of oxygen in sodium on niobium. A vanadium capsule was used, and tests were conducted for 500 hr at 600°C and 100 hr at 800°C. The results of these tests are listed in Table 3.

Table 3. Change in Weight and Oxygen Concentration of Vanadium Specimens Exposed to Sodium Containing Various Amounts of Oxygen

Temperature (°C)	Initial Oxygen Content of Sodium[a] (ppm)	Specimen Weight Gain[b] (mg)	Final Oxygen Content of Specimen[c] (ppm)
600	50	0.2	1900
	250	0.3	1900
	550	0.4	2100
	850	1.1	2200
	1300	1.6	2300
800	50	0.0	1900
	250	0.0	1900
	550	0.2	1900
	850	0.6	2000
	1250	1.1	2000

[a] Oxygen was added as Na_2O.

[b] Specimen dimensions: 1 × 0.5 × 0.040 in.

[c] Initial oxygen content of vanadium specimen was 1900 ppm.

The vanadium specimens gained weight in proportion to the amounts of Na_2O added to the sodium. An oxygen mass balance showed that during test, the vanadium specimen and capsule picked up essentially all the oxygen added to the sodium. The surfaces of the specimens exposed at 800°C showed no indication of external scale formation, but the two specimens exposed to the highest oxygen concentrations at 600°C darkened slightly.

Because of the large amount of oxygen picked up by the vanadium capsule, we sought a capsule material that would interact less with the oxygen interchange between the vanadium specimen and the sodium. Similar tests were therefore made at 600°C with capsules of molybdenum and type 304L stainless steel. Molybdenum was chosen because it was thought to be relatively inert to oxygen interactions; stainless steel was chosen because of its interest for the LMFBR.

Table 4 shows the change in weight and oxygen concentration of the vanadium specimens as a function of the amounts of Na_2O added to the sodium. Unlike in the all-vanadium system, where the external surfaces of specimens exposed to high-oxygen sodium darkened only slightly, the specimens in these latter tests had scales: black in the molybdenum capsules and dark gray in the stainless steel capsules.

The specimens from these tests were analyzed for oxygen by fast-neutron activation analysis before and after test, and some of the specimens were reanalyzed after the external scale was removed. In all cases, scale removal lowered the oxygen content, indicating that the scale contained oxygen. Measurement of specimen thickness before and after scale removal showed scale thicknesses to be about 0.0005 in. The measured changes in oxygen concentration in the specimens generally agree with the measured weight gains; that is, the percentage of the oxygen picked up by the vanadium specimens decreased as the oxygen concentration in sodium increased. The decrease was quite significant for the molybdenum capsules: the vanadium specimens picked up only 50% of the oxygen available from sodium containing 4000 ppm O and about 75% from sodium containing 2000 ppm O. For the stainless steel capsules, on the other hand, all capsules showed essentially all oxygen was recovered except for the capsule with 4000 ppm O, where 91% of the oxygen was recovered.

Table 4. Change in Weight and Oxygen Concentration of Vanadium Specimens Exposed to Sodium Containing Various Amounts of Oxygen at 600°C

Exposure (hr)	Initial Oxygen Content[a] of Sodium (ppm)	Oxygen Added (mg)	Specimen Weight Gain (mg)	Oxygen Concentration[b] in Vanadium, ppm		
				Before Test	After Test	
					With Scale	Without Scale
		Molybdenum Container				
100	2000	15.5	9.4	1240	4120	3310
200	1800	15.6	9.4	1240	4080	3360
300	1950	15.5	14.6	1220	5760	4740
400	1950	15.5	13.3	1330	5340	c
500	1800	15.5	14.6	1270	5780	c
500	50		1.3	1290	1420	1220
500	450	3.9	5.0	1230	2950	2720
500	1000	7.8	8.9	1290	4350	3700
500	4000	31.1	14.3	1300	6150	c
		Type 304 Stainless Steel Container				
100	2000	14.2	7.2	1220	4390	2930
200	2050	14.2	7.8	1310	4900	3200
300	2050	14.2	12.0	1270	6170	3910
400	2050	14.2	10.0	1250	5200	c
500	2050	14.2	11.2	1270	6210	c
500	50		0.5	1270	1470	1250
500	550	3.6	3.8	1220	3040	2340
500	1100	7.1	7.6	1310	4630	3440
500	4000	28.6	20.6	1190	9790	c

[a]Oxygen was added as Na_2O.

[b]Oxygen concentrations were determined by fast-neutron activation analysis.

[c]Specimen was sectioned for chemical analysis of the external film.

Attempts to determine the nature of the external scales by x-ray diffraction were unsuccessful, probably because the film was too thin. The vanadium specimens were analyzed to determine if there was dissimilar metal mass transfer from the capsules. The molybdenum concentration of the vanadium tested in molybdenum capsules increased to 500 to 700 ppm from less than 10 ppm, which indicates a considerable increase in the molybdenum content at the specimen surface, because little molybdenum can diffuse into the specimen at 600°C. The vanadium specimens exposed

to sodium in the stainless steel capsules contained about 200 ppm Fe and 100 ppm Ni, essentially the same as before test; chromium, carbon, and nitrogen also showed no change. The deposition of molybdenum on the specimen surface may account for the decrease in the percentage of oxygen recovered from the molybdenum capsules at the higher oxygen concentrations.

The sodium was analyzed after test to determine the concentration of vanadium and container metals present; the results are given in Tables 5 and 6. Again, molybdenum is present in the largest amounts, an especially interesting result since molybdenum is generally thought to be inert to liquid alkali metals. The addition of vanadium and oxygen to the system evidently alters the compatibility.

Metallographic examination revealed no microstructural changes of the vanadium specimens, although the microhardness increased because of the increased oxygen concentration. If a layer of molybdenum was deposited on the specimens exposed in the molybdenum capsules, it was too thin to be resolved in the optical microscope.

Table 5. Concentrations of Dissolved Metals in Sodium After Exposure of Vanadium in Molybdenum Capsules at 600°C

Exposure (hr)	Initial Oxygen Content of Sodium (ppm)	Concentration of Metal in Sodium, ppm	
		V	Mo
100	2000	12	230
200	1800	7	290
300	1950	8	240
400	1950	18	290
500	1800	32	
500	50	6	
500	450	5	
500	1000	8	
500	4000	68	

Table 6. Concentrations of Dissolved Metals in Sodium After Exposure of Vanadium in Stainless Steel Capsules at 600°C

Exposure (hr)	Initial Oxygen Content of Sodium (ppm)	Concentration of Metal in Sodium, ppm			
		V	Fe	Ni	Cr
100	2000	7	100	3	10
200	2050	13	130	2	90
300	2050	3	35	1	2
400	2050	12	95	3	8
500	2050	19			
500	50	0.2			
500	550	16			
500	1100	16			
500	4000	25			

Vanadium Alloys

To compare the effect of oxygen in sodium on the alloys of Table 2, p. 5, with that on unalloyed vanadium, specimens of each alloy and unalloyed vanadium were simultaneously exposed to sodium containing 2000 ppm O in type 304L stainless steel capsules. After test, all specimens showed weight gains and had black or dark brown scales of varying thicknesses; weight gains and changes in the oxygen concentrations of the specimens are given in Table 7. In all cases the weight gains could be accounted for by the change in oxygen concentration (i.e., the amount of weight gained was in good agreement with the weight of oxygen added to the sodium as Na_2O); this indicates that there was little or no mass transfer from the capsule. Surface scales were scraped from several of the specimens and analyzed by thermal neutron activation, but only vanadium and sodium were detected; Fe, Ni, and Cr were absent. Likewise, no change in carbon and nitrogen was detected.

The test materials were examined metallographically before and after the 600-hr exposure. For the unalloyed vanadium and the alloys with chromium and molybdenum, Fig. 2 shows no obvious effects of the exposure, only some grain growth, which is expected from the time at temperature. However, the alloys that contained titanium or zirconium developed a zone

Table 7. Oxygen Concentration of Vanadium and Vanadium Alloys Exposed to Sodium Containing 2000 ppm O at 600°C

Alloy	Exposure (hr)	Weight Change,[a] mg		Oxygen Concentration, ppm		
		Vanadium	Vanadium Alloy	Vanadium	Vanadium Alloy	
				After[b]	Before	After
V–5% Cr	100	7.1	4.9	5010	106	3850
	200	7.6	3.7	4630	130	3470
	300	6.5	3.8	4760		3280
	600	6.4	3.1	5060		3580
V–10% Cr	100	7.4	3.9	5390	89	2890
	200	8.1	3.3	5820	82	2840
	300	7.5	2.4	5310		2320
	600	9.1	3.2	6030		2810
V–15% Cr	100	9.1	2.4	6250	147	2280
	200	9.1	1.7	6360	123	1950
	300	10.3	1.3	6830		1740
	600	9.8	0.8	7080		1560
V–20% Ti	100	8.8	3.7	6220	840	3620
	200	7.7	3.4	5580		3640
	300	7.1	3.3	5200		4020
	600	6.8	4.3	4990	970	5070
V–15% Cr–5% Ti	100	8.7	0.9	6170	970	2780
	200	9.2	1.0	6220	1040	2950
	300	5.9	1.2	4150		2790
	600	7.1	1.8	4880		3100
V–1.3% Zr	100	5.6	5.1	3940	175	4510
	200	3.7	4.0	3030	110	3740
	300	5.0	5.8	4250	132	5000
	600	4.8	6.0	4020	121	5200
V–5% Zr	100	5.2	7.2	3910	228	5330
	200	4.5	6.7	3850	220	5220
	300	3.7	7.4	3600	212	5520
	600	3.6	7.5	3320	196	5670
V–20% Mo	100	5.4	2.2	4090	184	2830
	200	4.7	0.4	4120	134	2490
	300	6.9	1.5	5980	155	2910
	600	7.4	1.2	6470	133	2980
Vanstar 7	100	8.7	0.8	5850	940	3010
	200	11.0	1.4	6790	980	2800
	300	7.6	1.1	5230		2930
	600	10.5	1.7	5540		3110
Vanstar 8	100	7.2	4.8	4930	750	4340
	200	6.6	3.1	4780	800	3390
	300	6.9	3.2	5100		3520
	600	5.9	3.3	4430		3690
Vanstar 9	100	9.1	5.5	6420	1040	5010
	200	7.4	4.7	5330	1120	4360
	300	5.9	3.7	4650		4110
	600	7.9	3.8	6050		4230

[a]All specimens were 1 × 3/8 × 0.04 in.

[b]Oxygen concentration before test was approximately 80 ppm.

Y-108455

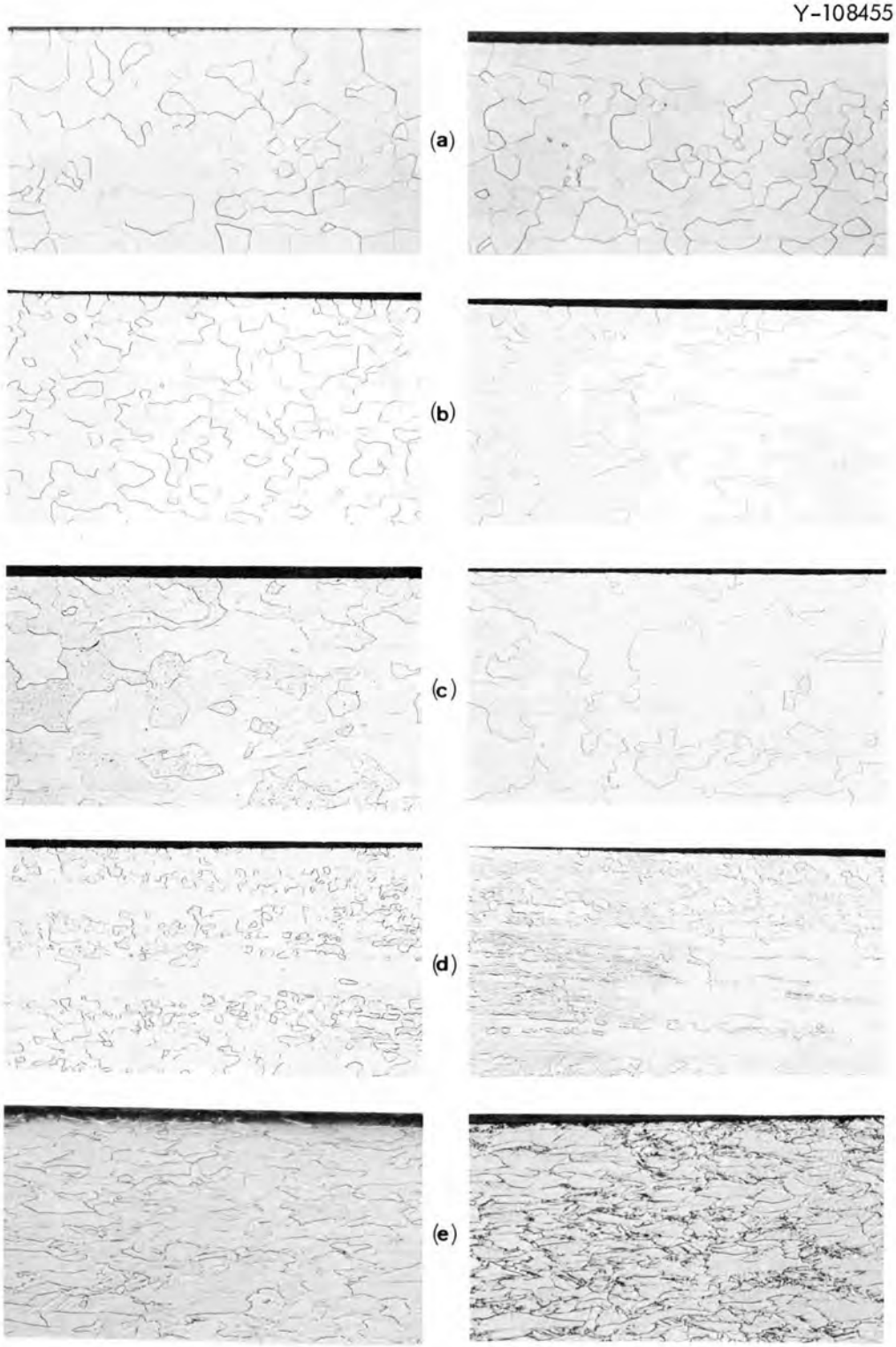

Fig. 2. Vanadium and Selected Alloys. Left: Before test, annealed 1 hr at 900°C. Right: After 600 hr at 600°C in sodium containing oxygen. Etched, 75×. (a) Unalloyed vanadium; (b) V–5% Cr; (c) V–10% Cr; (d) V–15% Cr; (e) V–20% Mo. Reduced 14%.

with different polishing and etching characteristics immediately below the external surface. This zone, which is caused by the internal oxidation of zirconium or titanium, is shown in Fig. 3 for etched specimens of alloys that showed shallow penetration depths. A greater penetration depth was observed in V–1.3% Zr, becoming nearly complete in 600 hr, as shown in Fig. 4. The appearance of the internally oxidized zone after

Y-108456

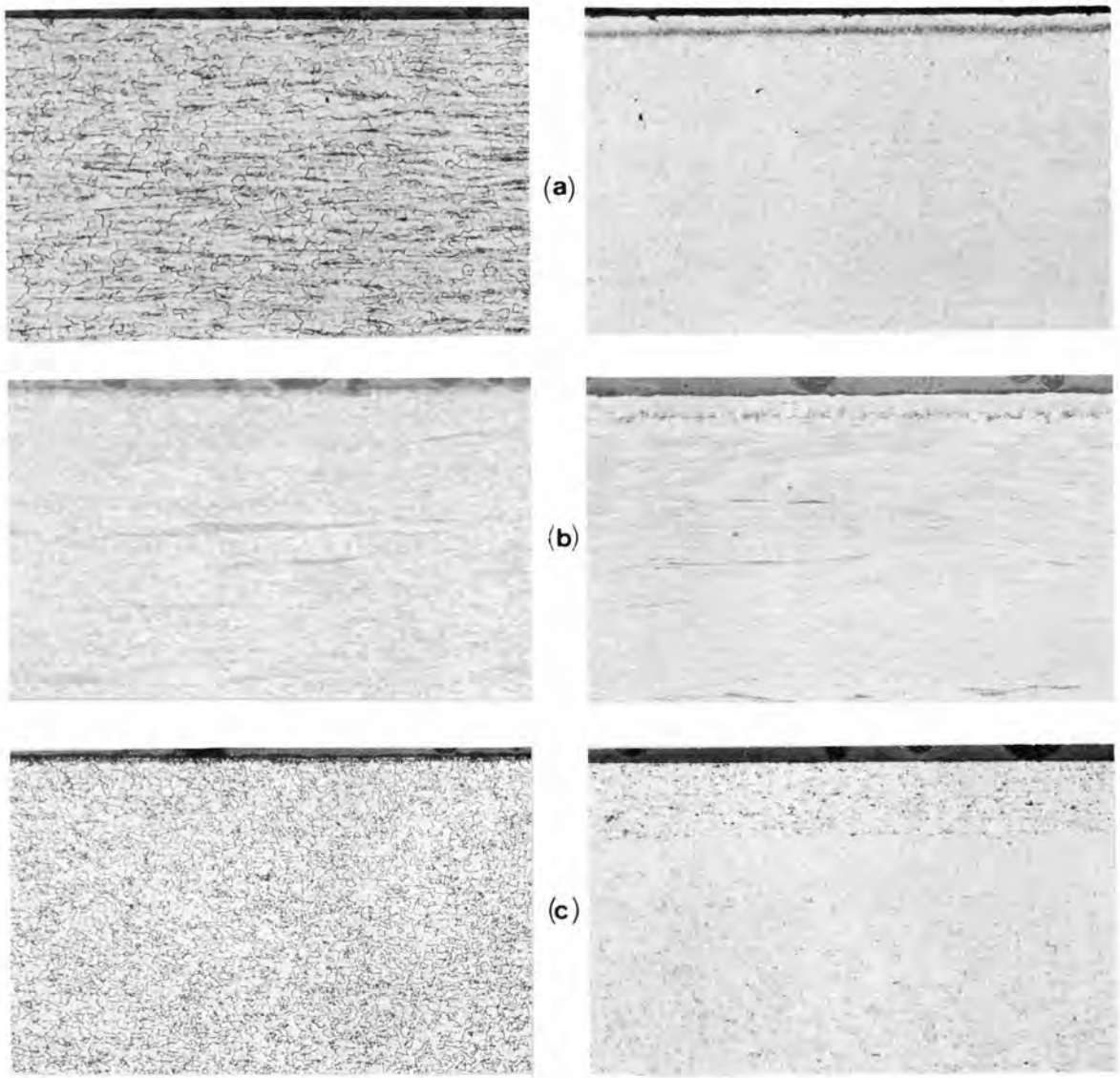

Fig. 3. Alloys with Shallow Internally Oxidized Zone. Left: Before test, annealed 1 hr at 900°C. Right: After 600 hr at 600°C in sodium containing oxygen. Etched, 75×. (a) V–20% Ti; (b) V–15% Cr–5% Ti; (c) V–5% Zr.

Y-108457

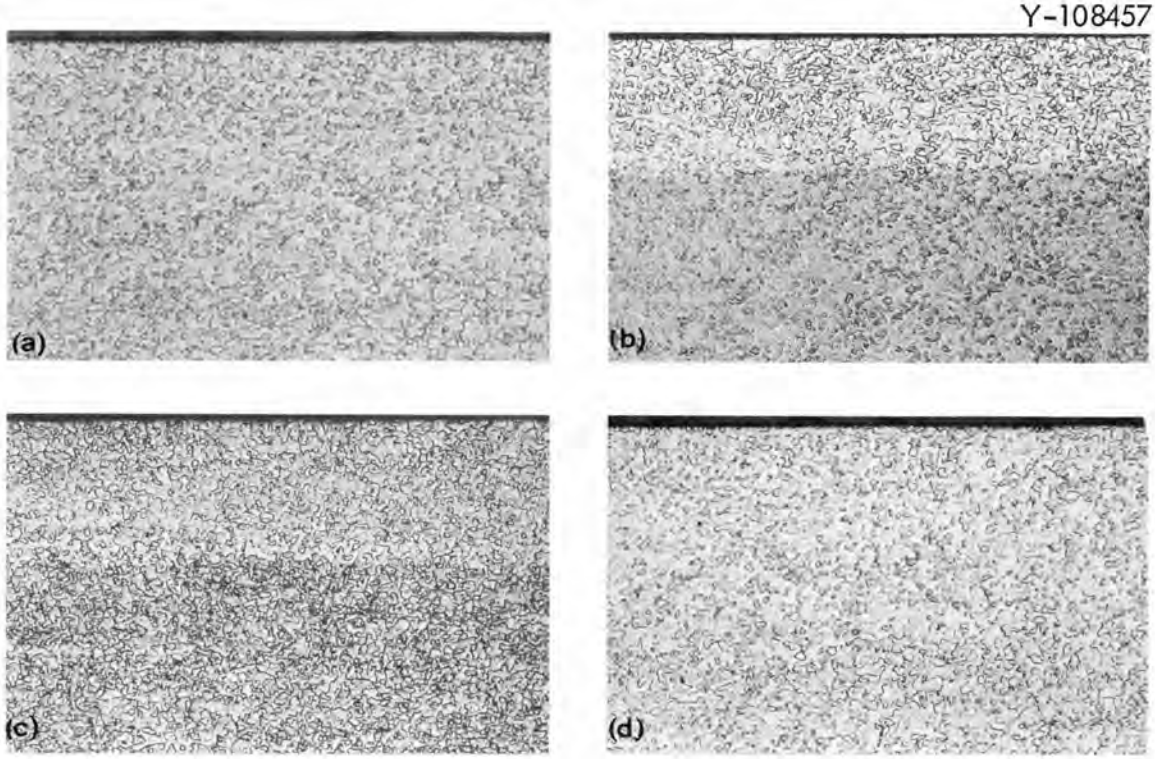

Fig. 4. Effect of Exposure Time on Penetration of V–1.3% Zr by Internal Oxidation Zone. Etched, 75×. (a) Before test, annealed 1 hr at 900°C. (b) After 100 hr, (c) 200 hr, and (d) 600 hr at 600°C in sodium containing oxygen.

polishing is shown in Fig. 5 for selected unetched specimens; this figure also shows the time dependence for V–5% Zr. Penetration depths as measured by a grain size eyepiece are given in Table 8.

Table 8. Depth of Internal Oxidation Zone, as Measured with a Grain Size Eyepiece

Exposure (hr)	Depth from Edge, μm			
	V–1.3% Zr	V–5% Zr	V–20% Ti	V–15% Cr–5% Ti
100	234	129	23	36
200	263	134		
300	373	147		
600	405	160	36	46

Y-108458

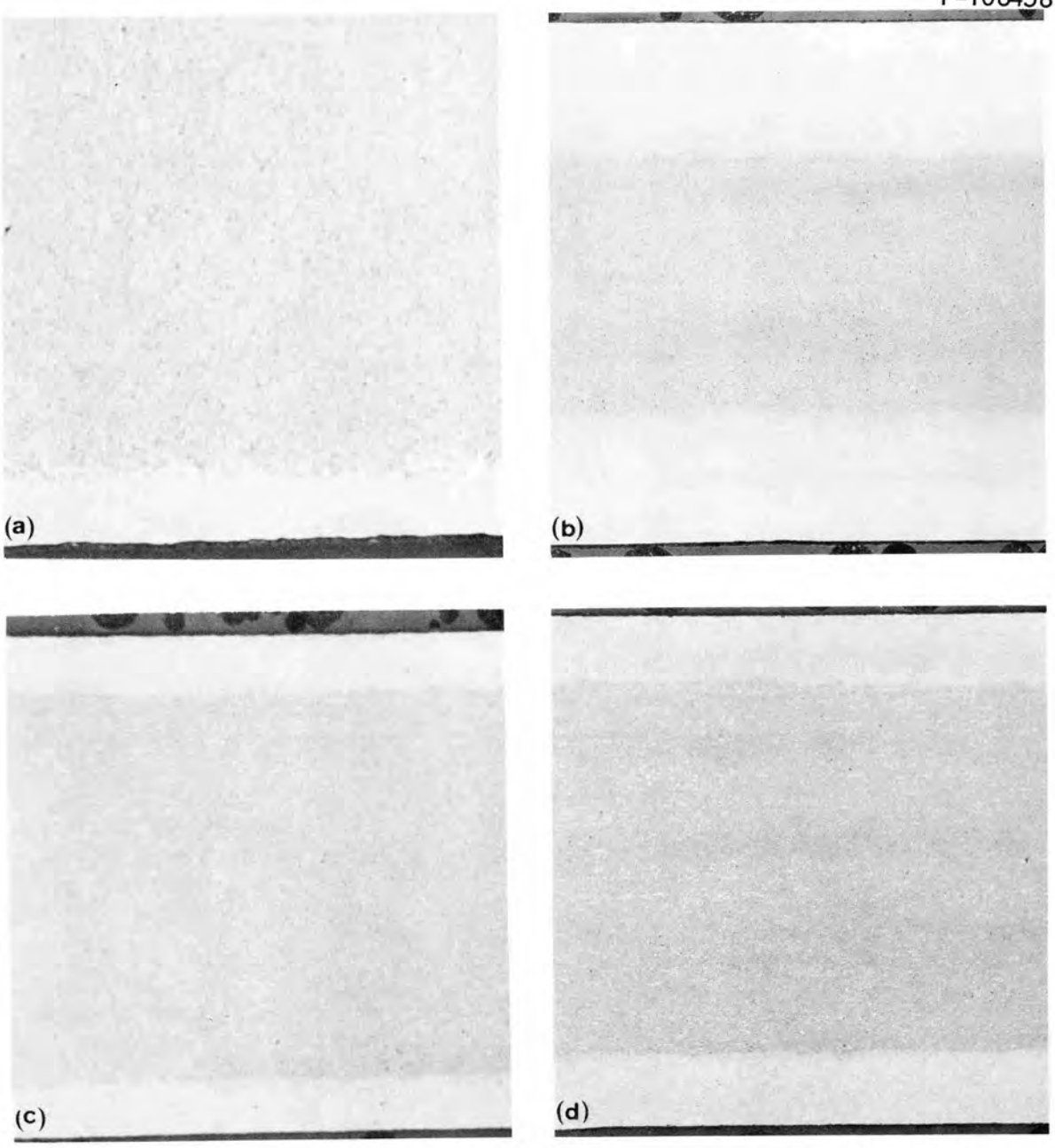

Fig. 5. The Internally Oxidized Zone as Seen in As-Polished Vanadium Alloy Specimens Exposed at 600°C to Sodium Containing Oxygen. (a) V–20% Ti exposed 600 hr, 500×. (b) V–1.3% Zr exposed 100 hr, 75×. (c) V–5% Zr exposed 100 hr, 75×. (d) V–5% Zr exposed 600 hr, 75×.

Although the Vanstar alloys also contain 1.3% Zr, the oxygen-affected zone was not easily detected metallographically, as seen in Fig. 6, probably because the preexisting precipitates in these alloys made any difference in etching characteristics difficult to detect.

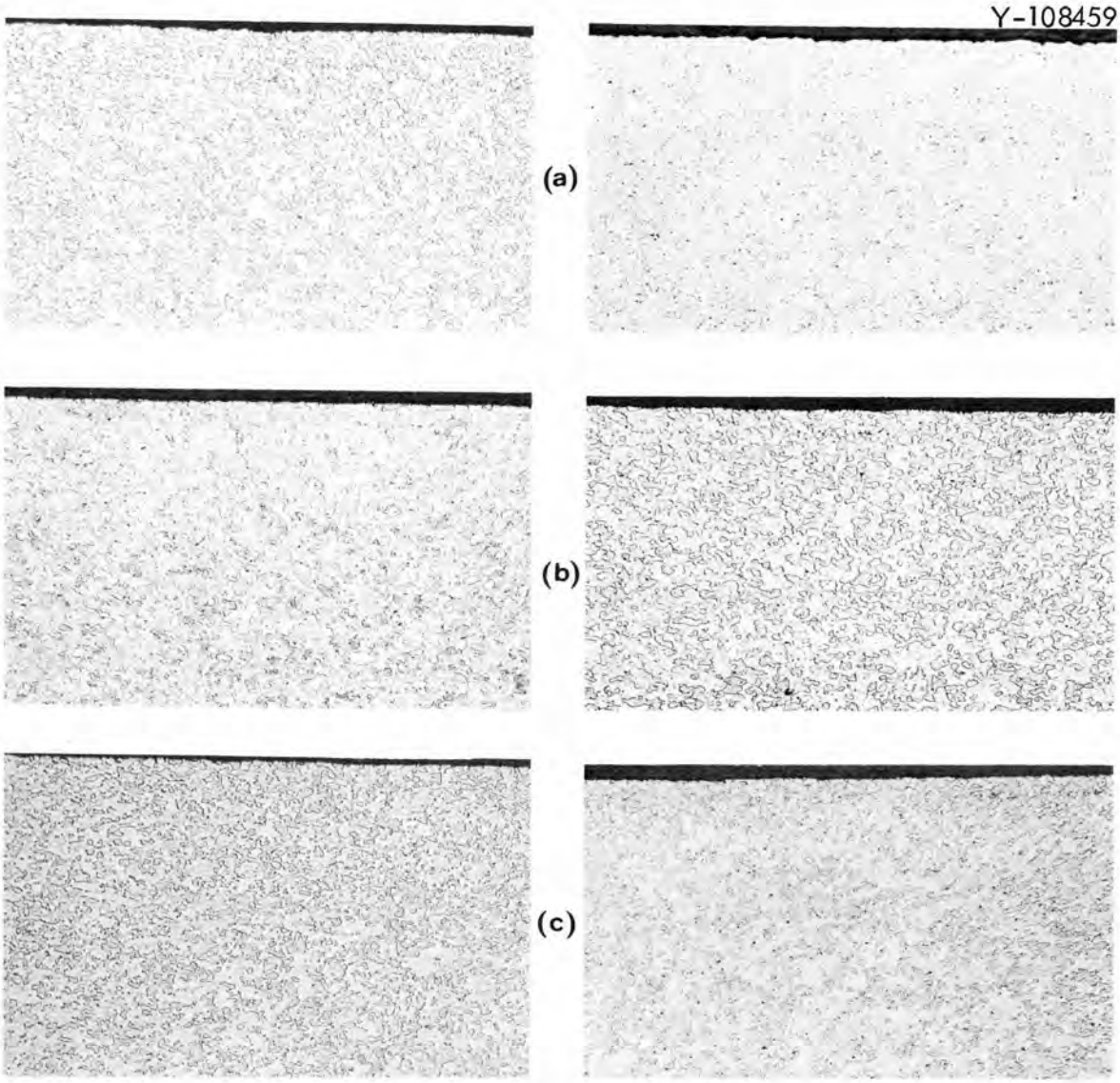

Fig. 6. Vanstar Alloys. Left: Before test, annealed 1 hr at 900°C. Right: After 600 hr at 600°C in sodium containing oxygen. Etched, 75×. (a) Vanstar 7. (b) Vanstar 8. (c) Vanstar 9.

When oxygen dissolves in vanadium or a vanadium alloy, the hardness increases, so the existence of an oxygen gradient can be determined from a microhardness profile. Table 9 lists the hardness profiles before test and after 100- and 600-hr exposures for the alloys that do not form internal oxides; Table 10 lists those that do. Because of variations in the hardness measurements, the results can be used for only qualitative

Table 9. Microhardness Profiles for Vanadium and Alloys that Do Not Oxidize Internally, Exposed to Sodium with 2000 ppm O at 600°C

Distance from Edge (μm)	Vickers Hardness Numbers (50-g Load)					
	Before Test	100 hr	600 hr	Before Test	100 hr	600 hr
	Vanadium[a]			V–5% Cr		
20	60	425	250	100	375	210
80	60	350	275	100	205	230
200	50	250	250	110	190	230
300	50	120	240	110	145	240
400		100	240		125	240
	V–10% Cr			V–15% Cr		
20	130	430	265	215	355	310
80	125	305	240	190	340	320
200	140	325	240	215	327	285
300	145	175	240	215	270	285
400		175			225	285
	V–20% Mo					
20	194	431	299			
80	194	326	299			
200	194	276	303			
300		255	299			
400		236	299			

[a]Vanadium specimens exposed with the V–15% Cr specimens.

conclusions. Table 9 shows that the non-internal-oxidizing alloys exposed to sodium for 100 hr have hardness gradients that disappear after 600 hr, indicating that equilibrium was reached in 600 hr. However, equilibrium is not approached in 600 hr for the V–20% Ti, V–15% Cr–5% Ti, and the vanadium-zirconium alloys (Table 10). An abrupt hardness change in going from the internal oxidation zone to the oxygen-unaffected zone is readily detected. Little or no gradient is detected for the Vanstar alloys after 600 hr.

Table 10. Microhardness Profiles for Vanadium Alloys that Oxidize Internally, Exposed to Sodium with 2000 ppm O at 600°C

Distance from Edge (μm)	Vickers Hardness Numbers (50-g Load)					
	Before Test	100 hr	600 hr	Before Test	100 hr	600 hr
	V–20% Ti			V–15% Cr–5% Ti		
20		720	1195		620	720
50	285	242	620	235	270	620
100	285	242	235	235	242	235
200	287	242	235	210	242	235
300	290	242	235	240	192	235
400		242				235
	V–1.3% Zr			V–5% Zr		
40	96	287	287	130	326	341
100	96	326	287	130	137	341
200	95	312	246	130	120	130
350	95	117	192	130	117	130
500		117	126		117	130
	Vanstar 7			Vanstar 8		
40	200	382	270	191	558	380
100	200	382	287	191	392	380
200	190	230	287	180	290	287
350	190	230	255	180	220	300
500		232	255		220	287
	Vanstar 9					
40		500	330			
100	226	430	330			
200	230	340	330			
350	230	265	299			
500		275	287			

DISCUSSION

Unalloyed Vanadium

A mass balance for oxygen in the tests that used vanadium capsules at 600 and 800°C showed that essentially all the oxygen added to the sodium was transferred to the vanadium specimens and capsules during test. The results at 600°C differ significantly from those obtained for niobium

under otherwise similar test conditions.[8] For example, niobium containing 70 ppm O acquired oxygen only when the oxygen concentration in the sodium exceeded 1000 ppm. Even then, the amount of oxygen transferred was only a small fraction of the total amount present in the sodium. Thus, the equilibrium distribution coefficient, defined as the ratio of oxygen in the vanadium (or niobium) to that in the sodium, is much greater for the vanadium-sodium system than for the niobium-sodium system.

The amount of vanadium present in the sodium after test was temperature dependent but independent of the amount of oxygen initially added to the sodium (approximately 40 and 200 ppm V at 600 and 800°C, respectively, Table 3, p. 6). This behavior also contrasts with the niobium-sodium system, where the niobium concentration in the sodium increased sharply with oxygen additions to the sodium.[8] One further distinction between vanadium and niobium or tantalum concerns the influence of the initial oxygen concentration of the solid. At oxygen concentrations as high as those initially present in the vanadium (1600 to 1900 ppm), niobium and tantalum at 600°C undergo rapid intergranular attack by sodium.[9] Vanadium, however, showed no evidence of sodium attack, a difference in behavior that probably reflects the difference in the solid solubility of oxygen in the materials. At 600°C, 1900 ppm O in niobium or tantalum is near to or above the solubility limit, whereas it is only about 20% of the solubility limit for vanadium.

The oxygen content of sodium after test was not determined directly, but by a mass balance calculation one can estimate the equilibrium distribution coefficient for oxygen between vanadium and sodium. For the tests in the stainless steel capsules, where all the oxygen was picked up by the specimen, we estimate that the distribution coefficient at 600°C approaches a value of 10^4, in good agreement with the more accurate determination of Smith and Kassner,[10] who found a value of 1.5×10^4. In contrast to the niobium-oxygen-sodium system,[8] the distribution coefficient for the vanadium-oxygen-sodium system is in order of magnitude agreement with the value calculated theoretically.

In the previous section we concluded that the molybdenum that had transferred to and deposited on the vanadium specimen surfaces may have led to the decreased oxygen pickup. If we assume that the 700 ppm Mo is

evenly deposited on the specimen surface, the thickness of the molybdenum layer would be about 0.3 μm. These results indicate that it may be useful to investigate the use of molybdenum coatings to protect vanadium from oxygen during sodium exposure.

Vanadium Alloys

For discussion, the vanadium alloys can be divided into two groups: (1) alloys that contain elements forming less stable oxides than vanadium, and (2) alloys that form more stable oxides than vanadium and thus oxidize internally.[5] Since zirconium and titanium form more stable oxides than vanadium, only the three chromium alloys and the V–20% Mo alloy are not capable of forming internal oxides.

Both the weight changes and the oxygen analyses reveal that chromium strongly affects the oxygen partitioning between sodium and the alloy. The V–5% Cr gained less oxygen than unalloyed vanadium, while the alloys with higher chromium gained progressively less (Table 7, p. 11). Note also that the V–15% Cr gained less oxygen at longer test times than at the shorter times, suggesting that oxygen redistributed between the alloy and the companion vanadium specimen. Mass balance calculations show that essentially all the oxygen initially in the sodium is picked up by the two specimens within the first 100 hr – probably by the formation of external oxides. Then, during the subsequent time at temperature, two processes occur: the oxygen diffuses into the two specimens and is redistributed between the vanadium and the alloy.

Both the hardness measurements (Table 8, p. 13) and calculations based on the diffusion rate of oxygen in vanadium at 600°C indicate that equilibrium for oxygen in the vanadium-chromium alloys and V–20% Mo is approached in 600 hr. Therefore, the results can be used to compare the equilibrium distribution coefficients for oxygen between sodium and these alloys with the corresponding coefficient for unalloyed vanadium. The distribution coefficient for the alloy is defined as

$$\kappa^{V\text{-}Cr} = C_O^{(V\text{-}Cr)}/C_O^{(Na)} \qquad (1)$$

and that for unalloyed vanadium as

$$\kappa^{V} = C_O^{(V)}/C_O^{(Na)} \tag{2}$$

where $C_O^{(V\text{-}Cr)}$, $C_O^{(V)}$, and $C_O^{(Na)}$ are the equilibrium weight fractions of oxygen in the alloy, vanadium, and sodium, respectively. Then, since the specimens are exposed to a common sodium phase,

$$\kappa^{V\text{-}Cr}/\kappa^{V} = C_O^{(V\text{-}Cr)}/C_O^{(V)} \quad . \tag{3}$$

Figure 7 shows the effect of chromium composition on the ratio of distribution coefficients as determined in these tests and compares the values with distribution coefficients reported by Kassner and Smith.[11]

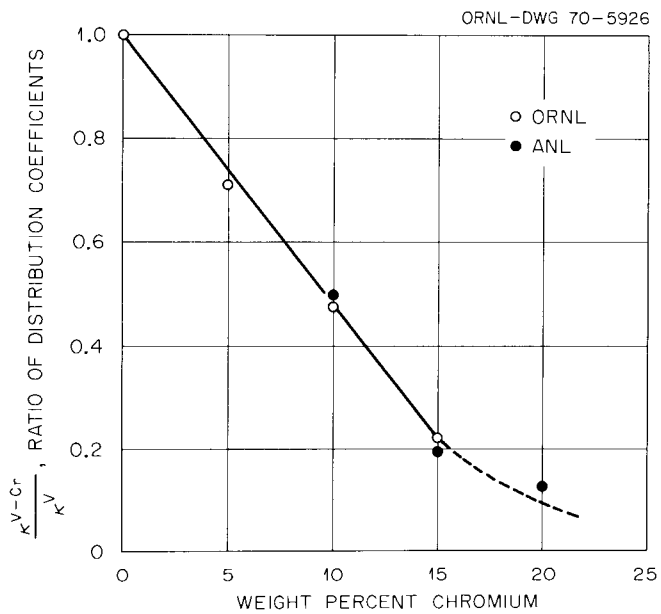

Fig. 7. The Effect of Chromium Concentration in Vanadium on the Distribution Coefficient for Oxygen Between Sodium and Vanadium at 600°C. ANL data taken from Kassner and Smith.[11]

The decrease in the distribution coefficient caused by chromium additions can be attributed to the effect of chromium on the solubility of oxygen in vanadium and can be described in terms of the effect of chromium on the activity coefficient of oxygen in vanadium. If the

standard state for oxygen in the two specimens is taken to be the same, then at equilibrium the activities are equal. Therefore,

$$\gamma_O^{(V\text{-}Cr)}/\gamma_O^{(V)} = N_O^{(V)}/N_O^{(V\text{-}Cr)} , \tag{4}$$

where the $\gamma_O^{(V\text{-}Cr)}$ and $\gamma_O^{(V)}$ are the activity coefficients for oxygen in the alloy and vanadium and $N_O^{(V\text{-}Cr)}$ and $N_O^{(V)}$ are the corresponding atom fractions of dissolved oxygen. Because vanadium and chromium have nearly the same atomic weight, the ratios of atom fractions and weight fractions are essentially equal. Therefore,

$$\gamma_O^{(V\text{-}Cr)}/\gamma_O^{(V)} \approx C_O^{(V)}/C_O^{(V\text{-}Cr)} , \tag{5}$$

and this ratio can be calculated from the data in Fig. 7 and Eq. (3).

We can introduce the interaction parameter formalism of Wagner[12] to represent the effect of chromium on the activity of oxygen in vanadium as

$$\ell n\ \gamma_O^{(V\text{-}Cr)} \approx \ell n\ \gamma_O^{(V)} + N_O^{(V)}\epsilon_O^{(O)} + N_{Cr}^{(V)}\epsilon_O^{(Cr)} , \tag{6}$$

where $\epsilon_i^{(j)}$ is the interaction parameter that empirically describes the interactions between the solutes present (all interactions higher than first order have been dropped). When Henry's law applies to the vanadium-oxygen binary, $\epsilon_O^{(O)} = 0$, and Eq. (6) can be rewritten as

$$\ell n\left[\gamma_O^{(V\text{-}Cr)}/\gamma_O^{(V)}\right] \approx N_{Cr}^{(V)}\epsilon_O^{(Cr)} . \tag{7}$$

The $\epsilon_O^{(Cr)}$ can be determined from the plot of $\ell n\left[\gamma_O^{(V\text{-}Cr)}/\gamma_O^{(V)}\right]$ [which equals $\ell n(C_O^{(V)}/C_O^{(V\text{-}Cr)})$] against N_{Cr} that is shown in Fig. 8. Equation (7) is obeyed (linear) up to $N_{Cr} \approx 0.1$, and

$$\epsilon_O^{(Cr)} \approx 7.5 , \quad 0 < N_{Cr} < 0.1 . \tag{8}$$

A similar explanation applies to the V–20% Mo alloy; that is, molybdenum decreases the solubility of oxygen in vanadium. For V–20% Mo, $\kappa^{V\text{-}Mo}/\kappa^{V} \approx 0.45$. Since 20 wt % Mo is about 11 at. %, comparison with Fig. 7 shows that equal atom fractions of molybdenum and chromium

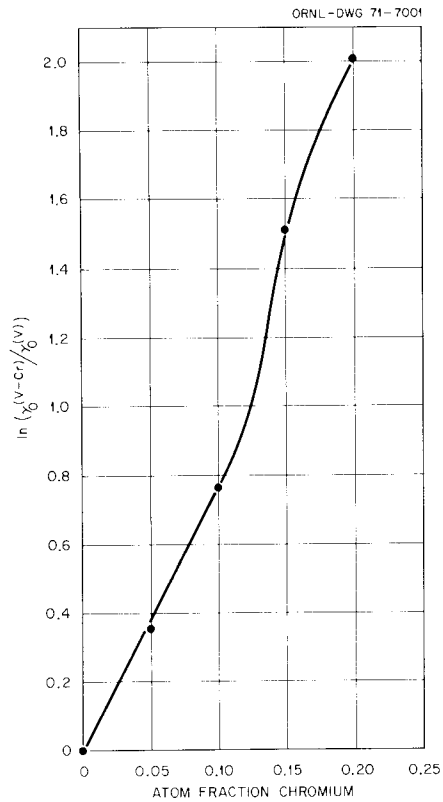

Fig. 8. The Effect of Chromium on the Activity Coefficient of Oxygen in Vanadium.

(both are Group VI A elements) affect the distribution coefficient and thus the solubility of oxygen similarly.

The V–20% Mo exposed to the sodium for 100 and 600 hr showed, in addition to the grain growth previously discussed, grain boundary cracking and the formation of small grains at the surface of the specimen on the edge perpendicular to the rolling direction (Fig. 9). No cracks or small grains (Fig. 10) were found in the material before test (as annealed), indicating that the cracks may be due to oxygen, the prolonged anneal at 600°C, or a combination of both.

Because of a more complicated oxygen absorption process for the alloys that oxidize internally, they are not in equilibrium after 600 hr at 600°C. During internal oxidation, oxygen diffuses into the alloy and reacts with the alloying element to precipitate an insoluble oxide at an advancing reaction front parallel to the external surface.

Y-108460

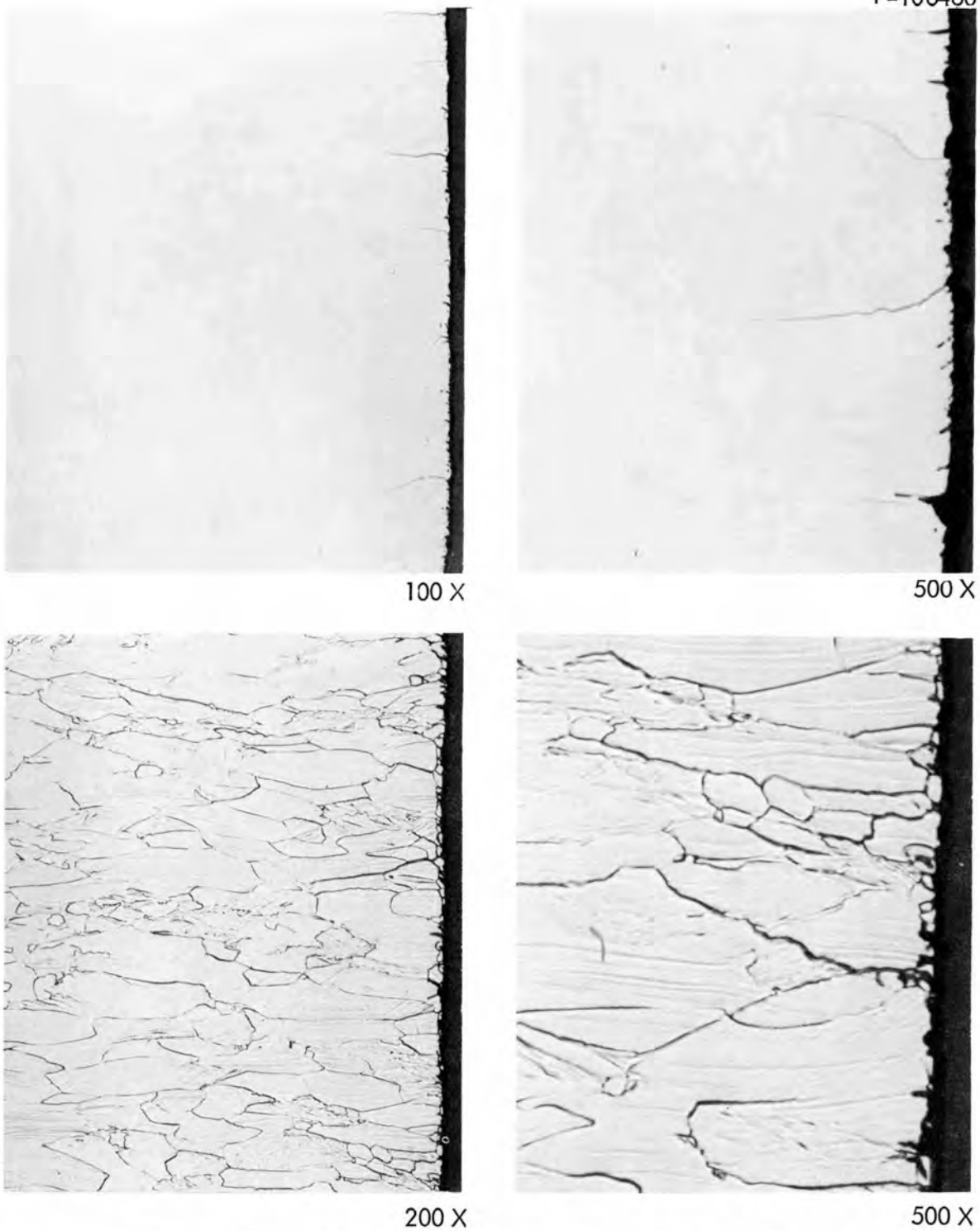

Fig. 9. The Edge of the V–20% Mo Specimen that Was Exposed to Sodium Containing Oxygen for 600 hr at 600°C. Top: Unetched, showing cracks. Bottom: Etched, showing cracks and small grains.

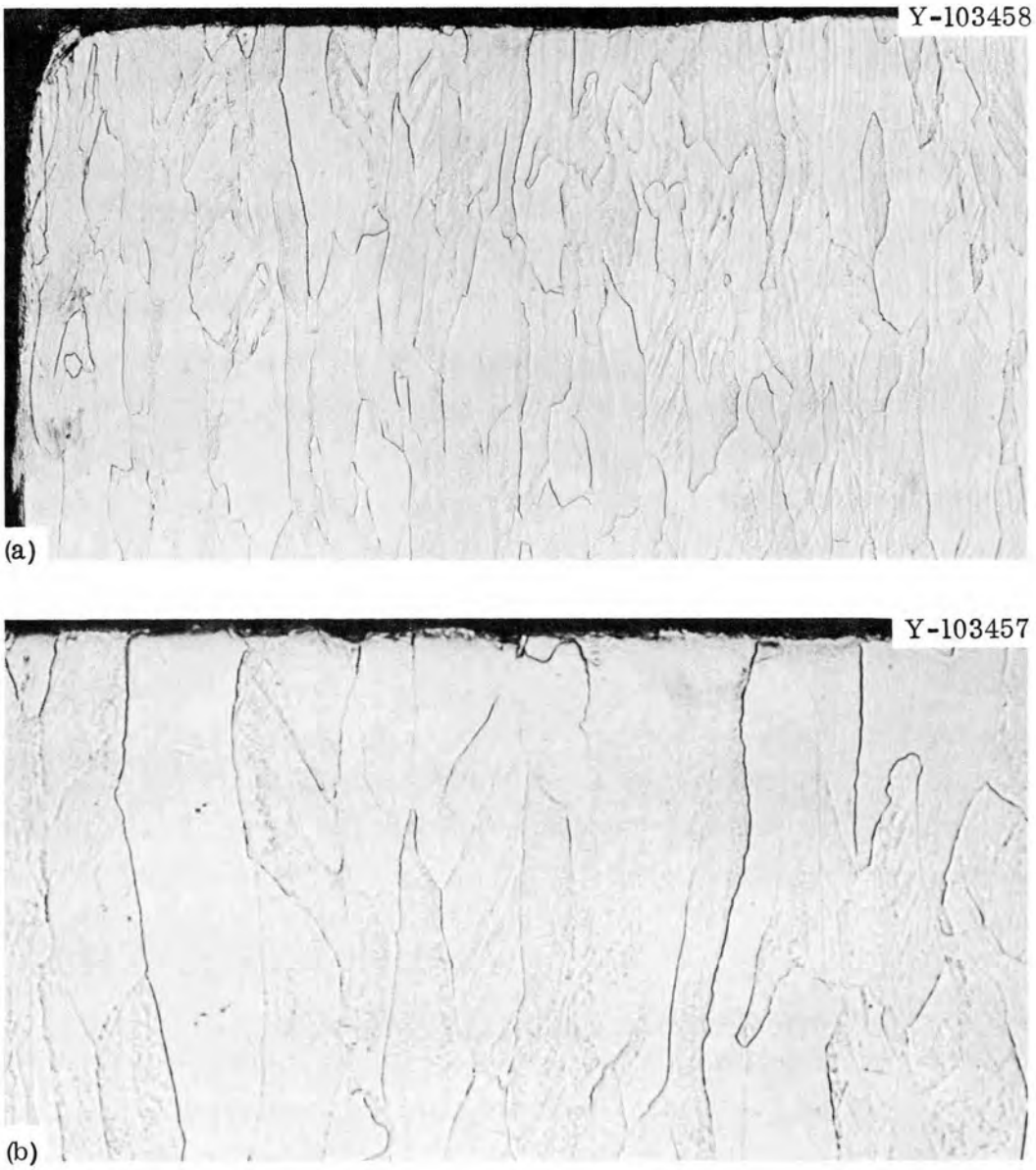

Fig. 10. Edge of V–20% Mo Before Test; Annealed 1 hr at 900°C. (a) 200×; (b) 500×.

Rapp[13] has reviewed the kinetics of internal oxidation as derived by Wagner[6] under the conditions of a constant surface concentration and no external scale formation. For the special case where the alloying element is oxidized in situ (i.e., only oxygen diffuses), the distance from the surface to the reaction front ξ (i.e., the depth of internal oxidation) is given by[13]

$$\xi = \left[2N_O^{(s)} D t_O / \nu N_B^{o}\right]^{\frac{1}{2}} , \qquad (9)$$

where $N_O^{(s)}$ is the concentration of oxygen in the alloy at the surface, N_B^{o} the concentration of the alloying component, D_O the diffusion coefficient of oxygen in the base metal, t the time, and ν the ratio of oxygen to metal atoms in the oxide precipitate.

Because of different boundary conditions, Eq. (9) is not directly applicable to the present studies; however, it can be used in a qualitative discussion of the results. The inverse dependence on the concentration of alloying component is obvious in Table 8, p. 13; note the increasing depths of penetration (at constant times) with decreasing zirconium or titanium. Compare also the depths of penetration for the two alloys that contain titanium, and note that although the V–20% Ti contains four times as much titanium as the V–15% Cr–5% Ti alloy, the penetration of the latter exceeds that for V–20% Ti to a lesser extent than expected from Eq. (9). This probably reflects the decrease in $N_O^{(s)}$ brought about by the addition of 15% Cr (chromium lowers the solubility of oxygen in vanadium, as discussed above).

Although the Vanstar alloys contain 1.3% Zr, the internal oxidation zone is not easily detected metallographically. Table 10, p. 19, however, shows definite indications of a hardened zone. Because of variations in hardness measurements, we cannot draw quantitative conclusions from such data. Nevertheless, if we compare the hardness profiles of Vanstar 8, Vanstar 9, and V–1.3% Zr, it appears that penetration is complete after 600 hr in the Vanstar alloys but not in the V–1.3% Zr alloy. The data for Vanstar 7 are unclear.

If we examine the weight changes and changes in oxygen concentration given in Table 7, p. 11, we find much less oxygen is picked up by the

Vanstar alloys than the vanadium specimens that simultaneously contacted the sodium and less than the amount picked up by the V–1.3% Zr. As opposed to the large amount of oxygen picked up by the V–1.3% Zr between 100 and 600 hr, very little oxygen was picked up by the three Vanstar alloys during this same time period. These observations indicate that internal oxidation for the Vanstar alloys is complete and these alloys are approaching equilibrium.

After all of the internal oxidation element – zirconium for the Vanstar alloys – is reacted, equilibrium between the alloy and the unalloyed vanadium will be reached by a redistribution of the remaining oxygen (oxygen not tied up as zirconium oxide) between the two specimens. The final oxygen concentration of the alloy will be that tied up in the oxide precipitate plus that in solution.

Table 7 shows that Vanstar 7 gained less weight and oxygen than either Vanstar 8 or Vanstar 9. Since the ratio of chromium atoms to other atoms in Vanstar 7 and Vanstar 8 is about equal, a first guess is that the increased pickup of oxygen by Vanstar 8 is due to tantalum. Because of the similarity of tantalum and niobium, we would suspect that the increased pickup in Vanstar 9 is due to the niobium. These changes, therefore, are an indication of the relative effect of chromium, tantalum, and niobium on the solubility of oxygen in vanadium (tantalum and niobium are present in equal atom percents in Vanstar 8 and Vanstar 9, respectively). That is, all three components decrease the solubility, but chromium is more effective than tantalum or niobium. Needless to say, this is but a guess, for it ignores carbon and requires that chromium and iron have essentially the same effect on the oxygen solubility in vanadium (Vanstar 9 contains iron, but no chromium).

In the above discussion of the Vanstar alloys, we have not explained the apparent change in either N_B^o or ν that, in accordance with Eq. (9), leads to the increased penetration rates for the Vanstar alloys. That is, if Cr, Fe, Ta, and Nb lower the oxygen solubility, $N_O^{(s)}$, then N_B^o or ν must also decrease if complete penetration is to occur more rapidly than it does in V–1.3% Zr. The effective N_B^o (i.e., the amount of zirconium available to form oxide) could be lowered if some zirconium

was tied up as zirconium carbide, thus making it unavailable for oxide formation.

The metallography of the vanadium-zirconium and V–20% Ti alloys shows several unusual features. The internal oxidation zone was usually not characterized by visible precipitates but was revealed as a zone that was harder and polished and etched differently than the oxygen-unaffected material. The inability to distinguish a precipitate phase is not too surprising, however, for at 600°C very little alloying element diffuses. Thus, the alloy oxidizes in situ, and small precipitate particles form. These small particles give rise to internal stresses, which cause the observed hardening in the oxygen-affected zone.

Figure 11 shows the before-test micrographs of the vanadium-zirconium alloys at high magnification. Both specimens contain precipitate before test (after a 1-hr anneal at 900°C). Comparison of the microstructures for the 1.3 and 5% Zr alloys indicates that much more precipitate phase is present in the 5% Zr. The V–5% Zr contains a blocky precipitate structure, compared to the much finer scale of precipitate present in the 1.3% alloy. These observations are contrary to the results of Baron et al.,[14] who reported that a 5% Zr alloy at 900°C should only contain a solid solution phase (i.e., the solubility of zirconium in vanadium at 900°C is greater than 5%); however, at 600°C, two phases,

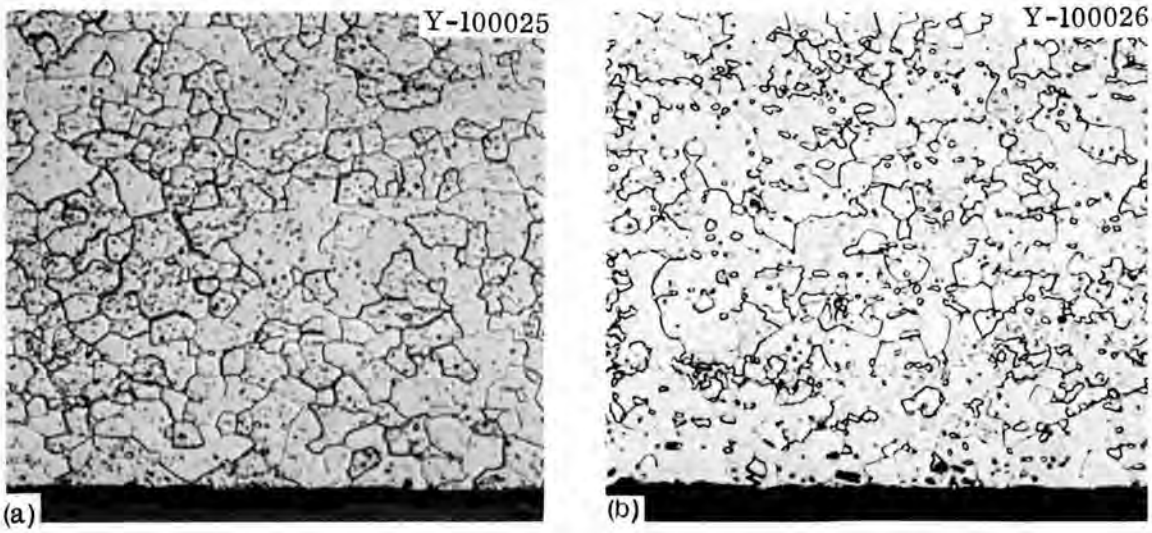

Fig. 11. Before-Test Microstructures of (a) V–1.3% Zr and (b) V–5% Zr. Annealed 1 hr at 900°C. Etched. 500×.

the vanadium-zirconium solid solution and a ZrV_2 intermetallic phase, should be present in the 5% alloy but not the 1.3% alloy.

With the exception of the different ecthing characteristics of the oxygen-affected zone, the microstructure for the 1.3% Zr alloy is not noticeably changed after test. Figure 12 shows the after-test microstructure of the V–5% Zr at high magnification; two zones, in this case, are differentiated, not only by the internal oxidation zone, but by the morphology of the precipitate phase in the oxygen-affected and oxygen-unaffected zones. A blocky second phase, which must be the ZrV_2 compound, is definitely present in the specimen center (oxygen-unaffected zone) in much larger percentages than was present before test. The oxygen-affected zone contains holes where the second phase either fell out during metallographic preparation or was oxidized simultaneously with the internal oxidation of the zirconium in solution. If a layer of zirconium oxide formed about the periphery of the ZrV_2, or if the ZrV_2 was completely oxidized, the oxide may have dissolved during metallographic preparation to give the observed holes. The oxidation of the zirconium in solution must affect the precipitate, for once all the zirconium in solution is oxidized, ZrV_2 will dissociate to reestablish equilibrium.

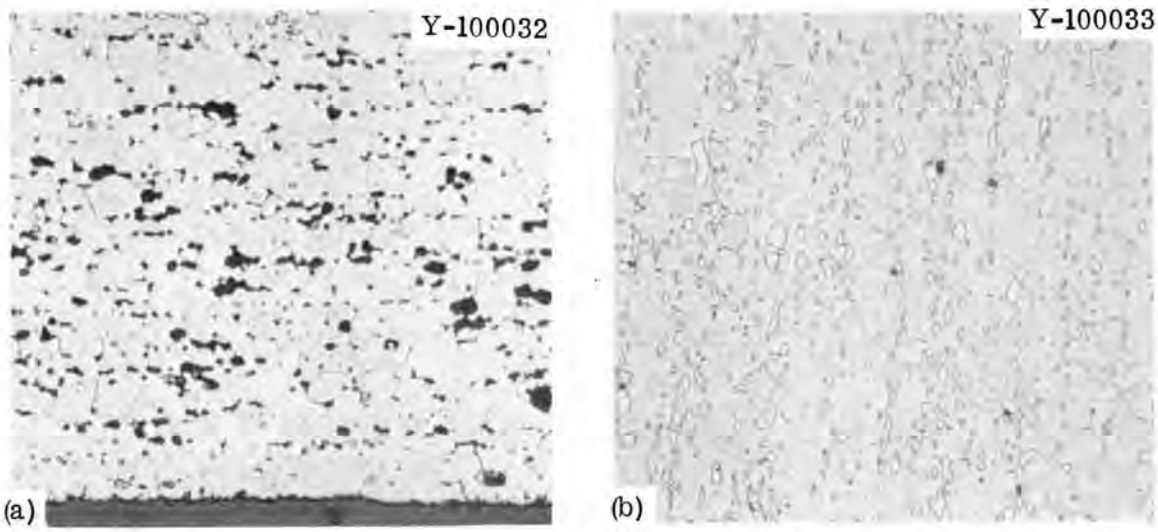

Fig. 12. Alloy V–5% Zr After 100 hr at 600°C. (a) Microstructure of both the oxygen-affected and oxygen-unaffected regions; (b) microstructure of the oxygen-unaffected region (specimen center). Etched. 500×.

Figure 13 shows the V–20% Ti alloy at high magnification before test and after a 600-hr exposure. Although a large amount of a fine precipitate phase is present before test, very noticeable changes occur as a result of the oxygen absorption. The oxygen-affected zone displays two regions: one is immediately adjacent to the external surface and appears to be free of precipitate; the second contains a high density of a fine precipitate phase. Observations similar to these have been made when vanadium-titanium alloys were oxidized in sodium[15] and oxygen at low pressures.[16]

In the gaseous tests, we found[16] that the second reaction zone begins to form (at the specimen surface) after the fine precipitate (internal oxidation) zone and then advances into the specimen by consuming the fine precipitate zone. Figure 14 shows the microstructure of V–20% Ti annealed 400 hr at 600°C at an oxygen pressure of 5×10^{-5} torr; a microhardness profile is superimposed and shows the extreme hardness of the second zone.

We feel this microstructure arises when oxygen diffuses into the alloy and reacts with the titanium to precipitate titanium oxide; this is the dense precipitate zone, the internal oxidation zone. As this zone moves into the specimen interior and depletes the titanium in solid

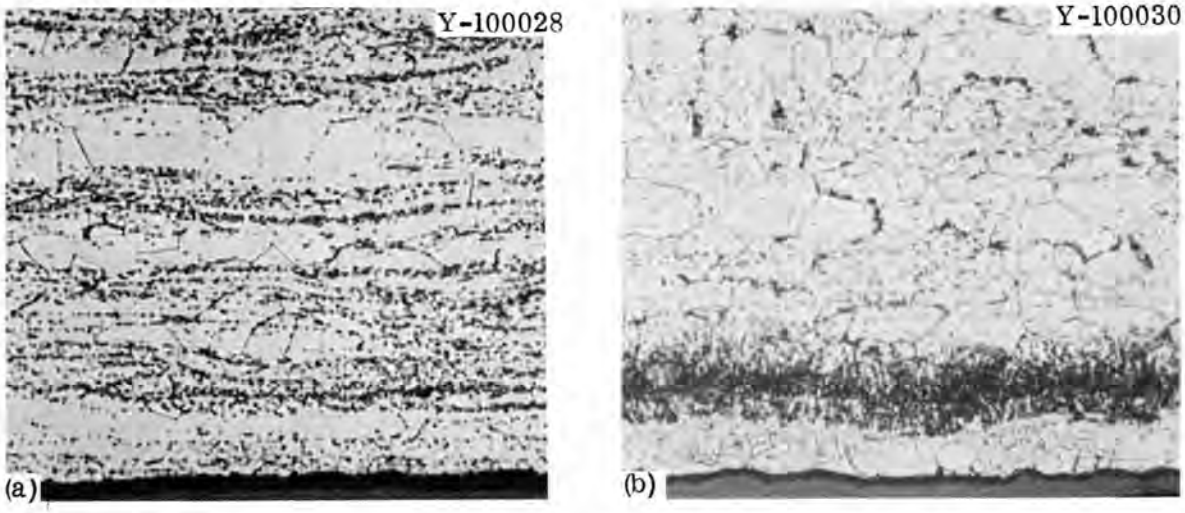

Fig. 13. Alloy V–20% Ti (a) Before Test and (b) After Exposure to Sodium Containing Oxygen for 600 hr at 600°C. Note the three different zones. Etched. 500×.

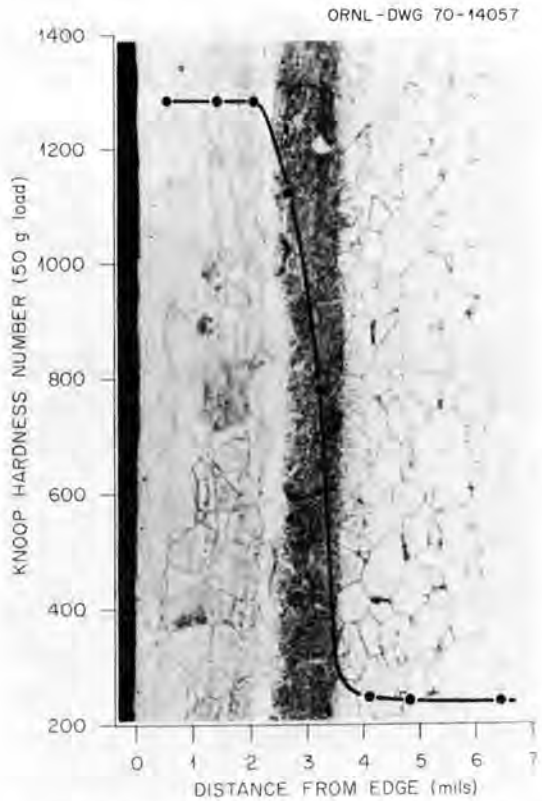

Fig. 14. Alloy V–20% Ti Exposed to Oxygen Gas for 400 hr at 600°C and 5×10^{-5} torr.

solution, oxygen will dissolve in the vanadium matrix of this zone. A concentration gradient develops between the specimen surface, where the oxygen concentration is determined by the oxygen concentration in the sodium or gas, and the precipitation front, where the oxygen concentration is essentially zero. Evidently, the oxygen concentration at the specimen surface is large enough to induce the phase transformation[17]

$$\alpha\text{-V (bcc s. solution)} \rightarrow \beta\text{-V (bct s. solution)} . \qquad (10)$$

The rate of advance of the α/β transformation front into the specimen interior is controlled by the rate of internal oxidation (dense precipitate region) and the rate of oxygen diffusion through the β region. Hardness measurements by Carlson and Alexander[18] on α and β solid solutions are consistent with the hardnesses measured for the inner and outer oxidation zones of the V–20% Ti (Fig. 14). Evidently the extreme hardness of the β phase somehow makes it impossible to resolve the oxide

precipitate in this region. The α/β phase transformation has not been observed for unalloyed vanadium similarly oxidized in a sodium or gaseous environment, an indication that the oxygen concentration for the transformation is lower in the vanadium-titanium system, possibly because of the internal stresses generated by the titanium oxide precipitate.

SUMMARY AND CONCLUSIONS

Vanadium and vanadium alloys getter oxygen from sodium. The equilibrium distribution coefficient for the partitioning of oxygen between unalloyed vanadium and sodium is greater than 10^4. For unalloyed vanadium, V–5% Cr, V–10% Cr, V–15% Cr, and V–20% Mo, oxygen dissolves in the matrix to form a solid solution. Both chromium and molybdenum lower the equilibrium distribution coefficient by lowering the oxygen solubility in vanadium.

The other alloys tested – V–20% Ti, V–15% Cr–5% Ti, V–1.3% Zr, V–5% Zr, and three Vanstar alloys – contained either titanium or zirconium and formed internal oxide precipitates. The interal oxidation zone moved into the specimen interior with time, was harder than the oxygen-unaffected zone, and was visible metallographically. We explained the observations with existing internal oxidation theory.

Major conclusions are:

1. Cr, Mo, Fe, Ta, and Nb lower the solubility of oxygen in vanadium; tantalum and niobium affect solubility to a lesser degree than chromium, molybdenum, and iron.

2. Alloys that contain either titanium or zirconium (and thus form an internal oxide) getter more oxygen than the same alloys without the titanium or zirconium. After internal oxidation, the oxygen is present in two forms: oxygen in the precipitated oxide and oxygen dissolved in the alloy matrix; the concentration of dissolved oxygen probably approaches the equilibrium solubility for the same alloy without the internal oxidation component (titanium or zirconium).

3. Internal oxide precipitates harden the lattice and thus embrittle the material.

4. It follows from (2) and (3) that vanadium alloys that contain titanium or zirconium are inferior to alloys without the titanium or zirconium for use in a sodium system.

ACKNOWLEDGMENTS

The authors wish to thank J. L. Griffith, Jr., for carrying out the experiments; C. E. Zachary for the metallography; S. Peterson, J. W. Koger, and O. B. Cavin for reviewing the manuscript; and Frances Scarboro for preparing the report.

REFERENCES

1. S. Greenberg, W. E. Ruther, and H. A. Lavin, p. 63 in Alkali Metal Coolants (Proceedings of a Symposium, Vienna, 28 November–2 December 1966), International Atomic Energy Agency, Vienna, 1967.

2. L. Champeix, R. Darras, and J. Sannier, ibid., p. 45.

3. H. U. Burgstedt and G. Frees, Corrosion 24, 209 (1968).

4. W. E. Ruther, p. 82 in Proceedings of the International Conference on Sodium Technology and Large Fast Reactor Design, November 7–9, 1968, ANL-7520, Part 1.

5. R. L. Klueh and J. H. DeVan, J. Less-Common Metals 22, 389–398 (1970).

6. C. Wagner, Z. Elektrochem. 63, 772 (1959).

7. R. A. Rapp and H. D. Colson, Trans. Met. Soc. AIME 236, 1616 (1966).

8. R. L. Klueh, pp. 171–176 in Proceedings of the International Conference on Sodium Technology and Large Fast Reactor Design, November 7–9, 1968, ANL-7520, Part 1.

9. R. L. Klueh, pp. 177–196 in Corrosion by Liquid Metals, ed. by J. E. Draley and J. R. Weeks, Plenum Press, New York, 1970.

10. D. L. Smith and T. F. Kassner, ibid., p. 137.

11. T. F. Kassner and D. L. Smith, p. 53 in Reactor Development Program Progress Report, December 1969, ANL-7655.

12. C. Wagner, Thermodynamics of Alloys, Addison-Wesley, Reading, Mass., 1952.

13. R. A. Rapp, Corrosion 21, 382 (1965).

14. V. V. Baron, Yu. V. Efimov, and E. M. Savitskii, Tr. Inst. Met. im. A. A. Baikova Akad. Nauk. SSSR 8, 278 (1961).

15. H. A. Lavin and S. Greenberg, An Exploratory Study of the Behavior of Niobium- and Vanadium-Base Alloys in Oxygen-Contaminated Sodium, ANL-6982 (January 1968).

16. R. L. Klueh, Metals and Ceramics Div. Ann. Progr. Rept. June 30, 1971, ORNL-4770, pp. 95–96.

17. J. L. Henry et al., J. Less-Common Metals 21, 115 (1970).

18. O. N. Carlson and D. G. Alexander, p. 15 in Reactor Materials Development Quart. Rept. January–March 1967, IS-RD-17.

ORNL-4739
UC-25 – Metals, Ceramics, and Materials

INTERNAL DISTRIBUTION

1–3. Central Research Library
4. ORNL – Y-12 Technical Library
Document Reference Section
5–24. Laboratory Records
25. Laboratory Records, ORNL RC
26. ORNL Patent Office
27. G. M. Adamson, Jr.
28. S. E. Beall
29. O. B. Cavin
30. R. E. Clausing
31. W. H. Cook
32. F. L. Culler
33. C. W. Cunningham
34. J. E. Cunningham
35–38. J. H. DeVan
39. J. R. DiStefano
40. R. G. Donnelly
41. B. Fleischer
42. A. P. Fraas
43. J. H Frye, Jr.
44. W. R. Grimes
45. A. G. Grindell
46. W. O. Harms
47. R. F. Hibbs
48–50. M. R. Hill
51. H. W. Hoffman
52. W. R. Huntley
53. H. Inouye
54–59. R. L. Klueh
60. J. W. Koger
61. J. M. Leitnaker
62. R. E. MacPherson
63. C. J. McHargue
64. H. E. McCoy, Jr.
65. A. J. Miller
66. P. Patriarca
67. R. E. Reed
68. A. C. Schaffhauser
69. J. L. Scott
70. D. B. Trauger
71. T. N. Washburn
72. A. M. Weinberg
73. J. R. Weir, Jr.
74. F. W. Wiffen
75. C. M. Adams, Jr. (consultant)
76. Leo Brewer (consultant)
77. Walter Kohn (consultant)
78. Jan Korringa (consultant)
79. Sidney Siegel (consultant)

EXTERNAL DISTRIBUTION

80. R. E. Anderson, Space Nuclear Systems Office, Washington, DC 20545
81. E. C. Bishop, Westinghouse Electric Corporation, P. O. Box 158, Waltz Mill Site, Madison, PA 15633
82. O. N. Carlson, Ames Laboratory, Iowa State University, P. O. Box 1129, Station A, Ames, IA 50010
83–84. E. G. Case, Director, Division of Reactor Standards, AEC, Washington, DC 20545
85. D. F. Cope, RDT, SSR, Oak Ridge National Laboratory
86. R. W. Davies, NASA Lewis Research Center, Plum Brook Station, Sandusky, OH 44870
87. G. K. Dicker, AEC, Washington, DC 20545
88. J. K. Elbaum, Code MAMP, Wright-Patterson Air Force Base, OH 45433
89. H. B. Finger, AEC, Washington, DC 20545

90. S. Greenberg, Argonne National Laboratory, 9700 South Cass Avenue, Argonne, IL 60439
91. D. H. Gurinsky, Brookhaven National Laboratory, 29 Cornell Avenue, Upton, Long Island, NY 11973
92. E. E. Hoffman, General Electric Company, P. O. Box 15132, Cincinnati, OH 45215
93. K. E. Horton, AEC, Washington, DC 20545
94. T. F. Kassner, Argonne National Laboratory, 9700 South Cass Avenue, Argonne, IL 60439
95. A. P. Litman, AEC, Washington, DC 20545
96. C. L. Matthews, RDT, OSR, AEC, Oak Ridge Naticnal Laboratory
97. J. M. McKee, Argonne National Laboratory, 970C South Cass Avenue, Argonne, IL 60439
98–100. Peter A. Morris, Director, Division of Reactor Licensing, AEC, Washington, DC 20545
101. H. Pearlman, Atomics International, P. O. Box 309, Canoga Park, CA 91304
102. W. E. Ray, Westinghouse Electric Corporation, Advanced Reactors Division, Waltz Mill Site, P. O. Box 158, Madison, PA 15633
103. N. Saunders, NASA Lewis Research Center, Plum Brook Station, Sandusky, OH 44870
104. C. M. Scheuermann, NASA Lewis Research Center, Plum Brook Station, Sandusky, OH 44870
105. J. M. Simmons, RDT, AEC, Washington, DC 20545
106. B. Singer, RDT, AEC, Washington, DC 20545
107. D. K. Stevens, RDT, AEC, Washington, DC 20545
108. J. A. Swartout, Union Carbide Corporation, 270 Park Avenue, New York, NY 10017
109. A. Van Echo, RDT, AEC, Washington, DC 20545
110. J. R. Weeks, Brookhaven National Laboratory, 29 Cornell Avenue, Upton, Long Island, NY 11973
111. M. J. Whitman, RDT, AEC, Washington, DC 20545
112–116. Executive Secretary, Advisory Committee on Reactor Safeguards, AEC, Washington, DC 20545
117. Laboratory and University Division, AEC, Oak Ridge Operations
118. Patent Office, AEC, Oak Ridge Operations
119–317. Given distribution as shown in TID-4500 under Metals, Ceramics, and Materials category (25 copies – NTIS)